Solid-State Synthesis, Crystal Structure, and Nonlinear Refractive and Absorptive Properties of the New Cluster $(n\text{-}Bu_4N)_2[MoOS_3Cu_3BrCl_2]$

Hongwei Hou,[†] Xiangrong Ye,[†] Xinquan Xin,*[,†] Jie Liu,[‡] Mingqin Chen,[‡] and Shu Shi*[,§]

State Key Laboratory of Coordination Chemistry, Department of Chemistry, Nanjing University, Nanjing 210008, China; Center of Analysis and Measurement, Fudan University, Shanghai 200043, China; and Optical Laboratory and Department of Chemical Engineering, National University of Singapore, Singapore 0511

Received June 8, 1994. Revised Manuscript Received December 13, 1994[⊗]

The title compound $(n\text{-}Bu_4N)_2[MoOS_3Cu_3BrCl_2]$ was synthesized for nonlinear optical studies by reaction of $(NH_4)_2MoO_2S_2$, CuCl, and $(n\text{-}Bu)N_4Br$ in the solid state. Single-crystal X-ray analysis reveals that the cluster anion assumes a nest-shaped structure. The crystal has a monoclinic symmetry with a space group of $P2_1/c$. Cell parameters are $a = 21.779(5)$ Å, $b = 11.169(7)$ Å, $c = 22.012(3)$ Å, $\beta = 118.61(1)°$, $V = 4700.7$ Å^3, and $Z = 4$. The crystal structure was refined to $R = 0.056$, $R_w = 0.058$. The cluster exhibits interesting self-defocusing and nonlinear absorptive properties. These nonlinear optical properties of the cluster and the electronic spectrum, XPS, and oxidation-reduction behavior of the cluster are discussed.

Introduction

NLO research in the last decade has been largely focused on semiconductors, conjugated polymers, and discrete organic molecules.[1] Recently, the fullerene C_{60} has also attracted much attention.[2] By contrast, inorganic clusters, a very promising group of compounds, have received little attention.[3] This is unfortunate because metal clusters may possess the combined strength of both organic polymers and semiconductors. The clusters are molecular and contain heavy atoms. Unlike the case of semiconductors where little structural modification can be implemented, both the skeleton and terminal elements of the clusters can be altered and/or removed so that alteration of NLO properties (such as self-focusing ⇌ self-defocusing interchange; change of relative importance of nonlinear refraction over nonlinear absorption) can be realized through structural manipulation. This aspect of metal clusters resembles that of organic molecules. The advantage that metal clusters have over most organic molecules is that they contain many heavy atoms. In this aspect they resemble semiconductors. Incorporation of heavy atoms introduces more sublevels into the energy hierarchy as compared to organic molecules with the same number of skeleton atoms, which permits more allowed electron transitions to take place and hence larger NLO effects. Incorporation of heavy atoms may be especially beneficial to NLO applications if linear absorption can be kept low. With metal clusters, this can be accomplished via proper choice of constituent elements, oxidation state, structural type, and peripheral ligands of the cluster. Preliminary progress has already been made toward this end.[4]

Recently, we discovered that some Cu-Mo(W)-S clusters exhibit very strong nonlinear optical (NLO) effects.[5-8] Among the clusters studied were $(n\text{-}Bu_4N)_3[MS_4M'_3BrX_3]$ (M = Mo, W; M' = Cu, Ag; X = Cl, Br, I),[5,6] $(n\text{-}Bu_4N)_2[MoOS_3Cu_3(NCS)_3]$,[7] and $(Et_4N)_4[Mo_2O_2S_6Cu_6Br_2I_4]$.[8] It was discovered that all of the cubic-cage-shaped Cu(Ag)-Mo(W)-S clusters, $(n\text{-}Bu_4N)_3[MS_4M'_3BrX_3]$, exhibit strong nonlinear absorption and negligibly small nonlinear refraction (self-focusing) while both the nest-shaped cluster $(n\text{-}Bu_4N)_2[MoOS_3Cu_3(NCS)_3]$ and the twin-nest-shaped cluster $(Et_4N)_4[Mo_2O_2S_6Cu_6Br_2I_4]$ exhibit a strong self-defocusing effect. Structurally, the nest-shaped MoS_3Cu_3 skeleton of the $(n\text{-}Bu_4N)_2[MoOS_3Cu_3(NCS)_3]$ cluster can be considered as a derivative (with one vertex, Br, missing) of the cubic-cage-shaped MoS_3Cu_3Br core of the $(n\text{-}Bu_4N)_3[MoS_4Cu_3BrX_3]$ clusters. However, a direct comparison between $(n\text{-}Bu_4N)_2[MoOS_3Cu_3(NCS)_3]$ and $(n\text{-}Bu_4N)_3[MoS_4Cu_3BrX_3]$ is hampered by the fact that the peripheral ligand sets of the

[†] Nanjing University.
[‡] Fudan University.
[§] National University of Singapore.
[⊗] Abstract published in *Advance ACS Abstracts,* February 1, 1995.

(1) (a) Chemla, D. S., Zyss, J., Eds. *Nonlinear Optical Properties of Organic Molecules and Crystals*; Academic: Orlando, 1987. (b) Huang, H., Ed. *Optical Nonlinearities and Instabilities in Semiconductors*; Academic: Boston, 1988.

(2) (a) Meth, J. S.; Vanherzeele, H.; Wang, Y. *Chem. Phys. Lett.* **1992**, *197*, 26. (b) K. Harigaya, K.; Abe, S. *Jpn. J. Appl. Phys.* **1992**, *31*, L887. (c) Ebbesen, T. W.; Tanigaki, K.; Kuroshima, S. *Chem. Phys. Lett.* **1991**, *181*, 501. (d) Wei, T. H.; Hagan, D. J.; Sence, M. J.; Van Stryland, E. W.; Perryand, J. W.; Coulter, D. R. *Appl. Phys. B* **1992**, *54*, 46.

(3) (a) Boggess, T. F.; Allan, G. R.; Rychnovsky, S. J.; Labergerie, D. R.; Venzke, C. H.; Smirl, A. L.; Tutt, L. W.; Kost, A. R.; McCahon, S. W.; Klein, M. B.; *Opt. Eng.* **1993**, *32*, 1063. (b) Murphy, D. M.; Mingos, D. M. P.; Forward, J. M. *J. Mater. Chem.* **1993**, *3*, 67. (c) Tutt, L. W.; McCahon, S. W. *Opt. Lett.* **1990**, *15*, 700. (d) Allan, G. R.; Labergerie, D. R.; Rychnovsky, S. J.; Boggess, T. F.; Smirl, A. L. *J. Phys. Chem.* **1992**, *96*, 6313.

(4) Shi, S.; Hou, H. W.; Xin, X. Q. *J. Phys. Chem.*, in press.

(5) Shi, S.; Ji, W.; Tang, S. H.; Lang, J. P.; Xin, X. Q. *J. Am. Chem. Soc.* **1994**, *116*, 3615.

(6) Shi, S.; Ji, W.; Lang, J. P.; Xin, X. Q. *J. Phys. Chem.* **1994**, *98*, 3570.

(7) Shi, S.; Ji, W.; Xie, W.; Chong, T. C.; Zeng, H. C.; Lang, J. P.; Xin, X. Q. *Mater. Chem. Phys.*, accepted.

(8) Hou, H. W.; Xin, X. Q.; Liu, J.; Chen, M. Q.; Shi, S. *J. Chem. Soc., Dalton Trans.* **1994**, 3211.

0897-4756/95/2807-0472$09.00/0

two clusters are also different (pseudo-halogen in the former vs halogen in the latter). It was not clear whether or not the difference of the peripheral ligand sets is an important contributor to the marked difference of NLO properties of the two series of clusters, even though a quick inspection of the relatively small influence on NLO behavior of the clusters caused by the change of peripheral ligands within the $(n\text{-}Bu_4N)_3[MS_4M'_3BrX_3]$ series already suggested a negative answer. Here, we report the solid-state synthesis and NLO properties of another cluster, $(n\text{-}Bu_4N)_2[MoOS_3Cu_3BrCl_2]$. This cluster has a single-nest-shaped structure and a set of peripheral ligands very similar to that of the cubic-cage-shaped $(n\text{-}Bu_4)_3[MoS_4Cu_3BrX_3]$. In this paper we also present the crystal structure, IR and electronic spectra, photoelectron spectrum, and oxidation–reduction behavior of the cluster.

Experimental Section

Reagents. The compound $(NH_4)_2MoO_2S_2$ was prepared as described in the literature.[9] The other chemicals were purchased as A.R. grade reagents and used without further purification.

Synthesis of $(n\text{-}Bu_4N)_2[MoOS_3Cu_3BrCl_2]$. A well-ground mixture of $(NH_4)_2MoO_2S_2$ (0.23 g, 1 mmol), CuCl (0.20 g, 2 mmol), and $(n\text{-}Bu)_4NBr$ (0.64 g, 2 mmol) was heated at 90 °C for 10 h under a nitrogen atmosphere. Extraction of the product with CH_2Cl_2 (20 mL) and filtration produced a deep red clean solution. Dropwise addition of 2-propanol (10 mL) to the top of the red solution produced a two-layer system from which red crystals (0.20 g) were obtained after standing for 1 week. The compound is insoluble in either ether or ethanol but soluble in CH_2Cl_2, THF, CH_3CN, and DMF. It shows characteristic infrared absorptions at 920 cm^{-1} ($\upsilon(Mo-O_t)$) and 444 cm^{-1} ($\upsilon(Mo-S_b)$). Anal. Calcd for $C_{32}H_{72}N_2BrCl_2Cu_3MoOS_3$: C, 37.16; H, 7.00; N, 2.71. Found: C, 37.54; H, 6.94; N, 2.68.

Crystal Structure Analysis. The molecular structure of $(n\text{-}Bu_4N)_2[MoOS_3Cu_3BrCl_2]$ was determined on an Enraf-Nonius CAD4 X-ray diffractometer. A summary of the crystal parameters and the intensity data collection details is given in Table 1.

The structure of the title compound was solved by direct methods. A total of nine atoms were located from an E-map prepared from the phase set with probability statistics. The remaining atoms were located in succeeding difference Fourier syntheses. Hydrogen atoms were included in the refinement but restrained to ride on the atom to which they are bonded. The final cycle of refinement included 240 variable parameters and converged with $R = 0.056$ and $R_w = 0.058$.

Other Structural Characterizations. Carbon, hydrogen, and nitrogen analyses were performed on a PE 240C elemental analyzer. Infrared spectra were recorded with a Fourier transform Nicolet FT-170SX spectrometer (KBr pellets). The electronic spectrum was measured on a Shimadzu UV-240 spectrophotometer. X-ray photoelectron spectral (XPS) data were obtained with an ESCALAB MK-II photoelectron spectrometer. Cyclic voltammograms were determined with a PN model 270 electrochemical analyzer. The electrochemical measurements were conducted in CH_3CN solutions containing 0.1 mol dm^{-3} of Et_4NClO_4 as the supporting electrolyte and using platinum as the working and the auxiliary electrodes under a nitrogen atmosphere. Reduction potentials were measured with reference to a standard hydrogen electrode.

Optical Measurements. An acetonitrile solution of $(n\text{-}Bu_4N)_2[MoOS_3Cu_3BrCl_2]$ was placed in a 1-mm quartz cuvette for optical limiting measurements. The compound is stable toward air and laser light. Its nonlinear optical response was measured with linearly polarized, 7-ns pulses from a Q-switched frequency-doubled Nd:YAG laser. The spatial profiles of the optical pulses ($\lambda = 532$ nm) were nearly Gaussian, and the light was focused onto the sample with a 25-cm focal-length focusing mirror. The spot radius of the laser beam was measured to be 35 ± 5 μm (half-width at $1/e^2$ maximum). The interval between the laser pulses was chosen to be ~5 s for operational convenience. The incident and transmitted pulse energies were measured simultaneously by two Laser Precision detectors (RjP-735 energy probes) which were linked to a computer by an IEEE interface.

An identical setup was adopted in the experiments to measure the Z-scan data, except that the sample was moved along the axis of the incident beam (Z- direction) with respect to the focal point instead of being positioned at its focal point.[5,6] An aperture of 0.5 mm radius was placed in front of the detector to assist the measurement of the self-defocusing effect.

Table 1. Experimental Details for $(n\text{-}Bu_4N)_2[MoOS_3Cu_3BrCl_2]$

Crystal Data	
empirical formula	$C_{32}H_{72}N_2MoOS_3Cu_3BrCl_2$
formula weight	1020.50
crystal system	monoclinic
space group	$P2_1/c$
a (Å)	21.779(5)
b (Å)	11.169(7)
c (Å)	22.012(3)
β (deg)	118.61(1)
V (Å^3)	4700.7
Z	4
D_c (g cm^{-3})	1.40
$F(000)$	2056
μ(Mo Kα), cm^{-1}	19.2
radiation	MoKα ($\lambda = 0.709\ 30$ Å)
T (K)	293
crystal size	$0.10 \times 0.12 \times 0.32$ mm
Intensity Measurements	
diffractometer	Enraf-Nonius CAD4
scan type	$\omega-2\theta$
$(2\theta)_{max}$	48.0°
takeoff angle	2.8°
scan rate	1–5°/min (in ω)
scan width	$0.7 + 0.350 \tan\theta$
no. of total reflections	8015
reflections with $I \geq 3\sigma(I)$	2585
no. of variables	240
corrections	Lorentz-polarization, linear decay (from 0.973 to 1.078 on I) empirical absorption based on Ψ-scans of seven reflections (from 0.83 to 1.00 on I)

Results and Discussion

Structure. The anionic cluster structure of the title compound is shown in Figure 1. Figure 2 depicts packing of the molecule in a unit cell. Positional and thermal parameters are listed in Table 2. Selected bond lengths and bond angles are collected in Tables 3 and 4, respectively.

The skeleton of the cluster, consisting of one Mo atom, three μ_3-S atoms, and three Cu atoms, is in a nest shape. The Mo atom is tetracoordinated by three bridging S atoms and one terminal O atom with S–Mo–S angles of 107.48(9)° and O–Mo–S angles of 112.0(2)°, respectively. Compared to free $[MOS_3]^{2-}$ (M = Mo, W) ions, the $MoOS_3$ fragment in $[MoOS_3Cu_3BrCl_2]^{2-}$ deviates slightly from C_3 symmetry while the distortion of the $MoOS_3$ fragments in $[MoOS_3Cu_3(NCS)_3]^{2-}$ is much more severe. For comparison, the crystal and bonding parameters of several nest-shaped clusters are given in Table 5. The local symmetry of the $MoOS_3$ moiety is also approximately C_3 in a recently synthesized twin-nest-shaped complex $(Et_4N)_4[Mo_2Cu_6O_2S_6Br_2I_4]$[8] (where

(9) Mecloneld, J. W.; Friesen, G. D.; Rosenhein, C. D.; Newton, W. E. *Inorg. Chim. Acta* **1983**, *72*, 205.

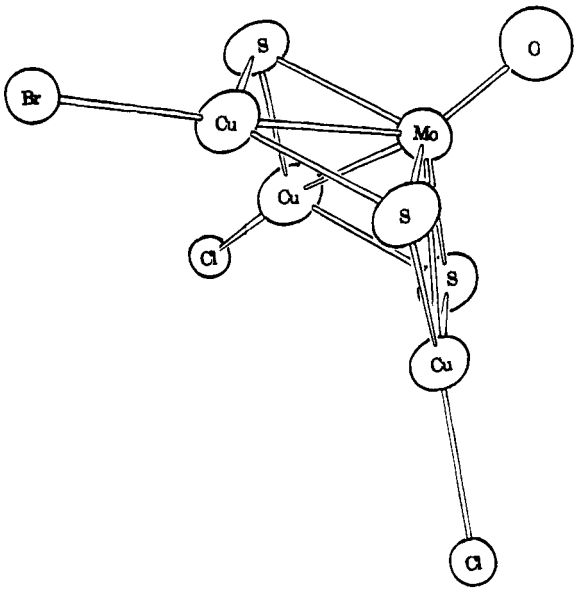

Figure 1. ORTEP diagram of the cluster anion of $(n\text{-}Bu_4N)_2[MoOS_3Cu_3BrCl_2]$.

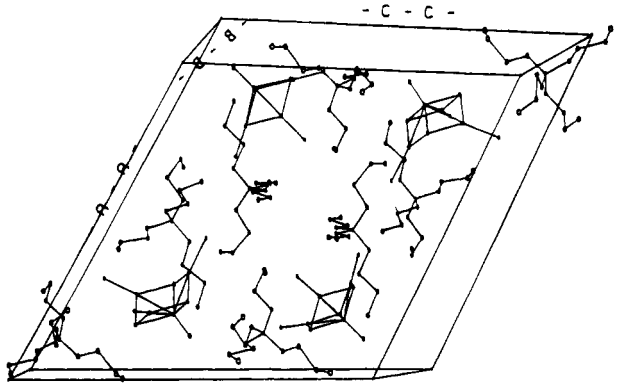

Figure 2. Packing scheme of a $(n\text{-}Bu_4N)_2[MoOS_3Cu_3BrCl_2]$ crystal.

Table 2. Positional Parameters and Their Estimated Standard Deviations of $(n\text{-}Bu_4N)_2[MoOS_3Cu_3BrCl_2]$

	X	*Y*	*Z*	B_{eq}
Mo	0.1847(7)	0.1139(2)	0.1825(7)	5.45(4)
Cu(1)	0.3073(9)	0.0320(2)	0.2074(9)	5.38(5)
Cu(2)	0.2507(1)	0.2357(2)	0.2989(1)	5.83(5)
Cu(3)	0.1787(1)	−0.0623(2)	0.2586(1)	6.63(6)
S(1)	0.2833(2)	0.2235(4)	0.2168(2)	5.9(1)
S(2)	0.1526(2)	0.1296(4)	0.2659(2)	6.2(1)
S(3)	0.2125(2)	−0.0801(4)	0.1777(2)	6.3(1)
O	0.1214(6)	0.158(1)	0.1057(6)	9.3(4)
Cl(1)	0.3986(2)	−0.0469(5)	0.2037(2)	4.4(1)
Cl(2)	0.2827(5)	0.355(1)	0.3778(5)	5.7(3)
Br	0.1825(2)	−0.2177(4)	0.3292(2)	7.0(1)
N(1)	0.4278(5)	0.639(1)	0.4369(5)	4.3(3)
N(2)	−0.1239(6)	−0.017(1)	0.0735(6)	6.5(4)
C(1)	0.3703(6)	0.636(1)	0.2751(6)	4.6(3)
C(2)	0.3008(7)	0.591(2)	0.2660(7)	6.3(4)
C(3)	0.2479(8)	0.574(2)	0.1878(8)	7.4(5)
C(4)	0.1772(9)	0.534(2)	0.176(1)	10.7(7)
C(17)	−0.0898(9)	0.042(2)	0.0343(9)	9.2(6)
C(18)	−0.071(1)	0.176(2)	0.048(1)	13.2(9)
C(19)	−0.051(1)	0.215(3)	−0.011(1)	15(1)
C(20)	−0.029(2)	0.332(3)	0.009(2)	24(2)

Mo−S bond lengths are 2.250(4), 2.261(4), and 2.272(4) Å; and S−Mo−S angles are 107.2(2)°, 107.9(2)°, and 108.1(2)°). The Mo−O bond length of 1.663(7) Å in the title cluster is typical for a double bond. The three Mo−S bond distances, 2.262(2)−2.266(2) Å, are in the range of single bonds. In comparison, the Mo atom in

Table 3. Selected Bond Lengths (Å) of $(n\text{-}Bu_4N)_2[MoOS_3Cu_3BrCl_2]$[a]

Mo−Cu(1)	2.621(1)	Mo−Cu(2)	2.638(1)
Mo−Cu(3)	2.628(1)	Mo−S(1)	2.265(2)
Mo−S(2)	2.262(2)	Mo−S(3)	2.266(2)
Mo−O	1.663(7)	Cl(1)−Cu(1)	2.212(4)
Cl(2)−Cu(2)	2.04(2)	Br−Cu(3)	2.305(3)
Cu(1)−S(1)	2.234(2)	Cu(1)−S(3)	2.230(3)
Cu(2)−S(2)	2.239(3)	Cu(2)−S(1)	2.241(2)
Cu(3)−S(3)	2.238(2)	Cu(3)−S(2)	2.243(2)
N(1)−C(1)	1.481(8)	N(1)−C(5)	1.527(9)
N(2)−C(17)	1.53(2)	C(1)−C(2)	1.512(9)
C(2)−C(3)	1.57(2)	C(19)−C(20)	1.40(2)

[a] Numbers in parentheses are estimated standard deviations in the least significant digits.

Table 4. Selected Bond Angles (deg) of $(n\text{-}Bu_4N)_2[MoOS_3Cu_3BrCl_2]$[a]

Cu(1)−Mo−Cu(2)	87.14(4)	Cu(1)−Mo−S(1)	53.82(7)
Cu(1)−Mo−S(2)	122.52(7)	Cu(1)−Mo−S(3)	53.69(7)
Cu(1)−Mo−O	125.4(2)	Cu(2)−Mo−O	129.6(2)
Cu(3)−Mo−O	126.7(2)	S(1)−Mo−S(2)	107.48(9)
S(1)−Mo−S(3)	107.48(9)	S(1)−Mo−O	111.9(2)
S(2)−Mo−S(3)	107.77(9)	S(2)−Mo−O	112.0(2)
S(3)−Mo−O	110.0(2)	Mo−Cu(1)−Cl(1)	167.3(4)
Mo−Cu(2)−Cl(2)	166.9(8)	Mo−Cu(3)−Br	175.7(1)
Mo−S(1)−Cu(1)	71.26(7)	Cu(1)−S(1)−Cu(2)	108.15(9)
S(1)−Cu(1)−S(3)	109.86(9)	S(1)−Cu(2)−S(2)	109.1(1)
S(2)−Cu(3)−S(3)	109.46(9)	C(1)−N(1)−C(5)	111.9(5)
N(1)−C(1)−C(2)	116.3(6)		

[a] Numbers in parentheses are estimated standard deviations in the least significant digits.

the $(n\text{-}Bu_4N)_3[MS_4M'_3BrX_3]$ series is coordinated by four S atoms. The three Mo−S_b bond lengths in the $(n\text{-}Bu_4N)_3[MS_4M'_3BrX_3]$ clusters are typically around 2.70 Å, about 0.34 Å longer than the Mo−S_b bonds in nest-shaped clusters. This difference in Mo−S bond lengths is largely caused by the difference in coordination environment of the Cu atoms in the two series.

All three Cu atoms in the title cluster adopt a trigonal planar coordination geometry with the sum of bond angles of one S−Cu−S and two S−Cu−X (X = Cl, Br) for each Cu atom ranging from 357.9° to 359.73°. The Cu atoms are linked to Mo through symmetrical Cu-$(S)_2$S bridges with all Cu−S distances in a range 2.230(3)−2.243(2) Å. This triangular coordination geometry differs significantly from the tetrahedral coordination geometry adopted by all of the Cu atoms in the $(n\text{-}Bu_4N)_3[MS_4Cu_3BrX_3]$ series and allows formation of stronger π-bonding over the Mo$(S)_2$Cu ring.

Electronic Spectra, XPS, and Cyclic Voltammogram. Figure 3 gives the linear absorption spectrum of the title compound, showing characteristic absorption bands at 500, 408, and 286 nm which are roughly comparable to the absorption bands of $MoOS_3^{2-}$ at υ_1 = 465 nm ($1a_2 \rightarrow 6e$), υ_2 = 392 nm ($5e \rightarrow 6e$), υ_3 = 313 nm ($1a_2 \rightarrow 7e$).[10,11] Because strong S → Mo charge transfer bands are significantly affected by the coordination of $MoOS_3^{2-}$ to Cu atoms, shifting of electronic transition bands are observed. The longest-wavelength band υ_1 is strongly shifted to longer wavelengths (465 → 500 nm) due to this coordination, whereas υ_3 is shifted to shorter wavelengths (313 → 286 nm).

Assessment of oxidation states of constituent elements is important not only to the interpretation of the

(10) Diemann, E.; Muller, A. *Spectrochim. Acta* **1970**, *26A*, 215.
(11) Muller, A.; Diemann, E.; Neumann, F.; Mengem, R. *Chem. Phys. Lett.* **1972**, *16*, 521.

Table 5. Comparison of Crystal and Bonding Parameters among Selected Clusters

$[MoOS_3Cu_3BrCl_2]^{2-}$ (I)	$[MoOS_3Cu_3Cl_3]^{2-}$ (II)	$[MoOS_3Cu_3(NCS)_3]^{2-}$ (III)	$[WOS_3Cu_3Cl_3]^{2-}$ (IV)
monoclinic $P2_1/c$	monoclinic $P2_1/a$	monoclinic $P2_1/n$	monoclinic $P2_1/a$
a = 21.779(5) Å	a = 16.932(3) Å	a = 16.672(9) Å	a = 16.941(3) Å
b = 11.169(7) Å	b = 12.676(3) Å	b = 16.278(6) Å	b = 12.691(2) Å
c = 22.012(3) Å	c = 17.626(3) Å	c = 19.608(8) Å	c = 17.634(3) Å
β = 118.61(1)°	β = 98.60(1)°	β = 110.05(4)°	β = 93.55(2)°
V = 4700.7 Å^3	V = 3776(3) Å^3	V = 4999 Å^3	V = 3784(4) Å^3
Z = 4	Z = 4	Z = 4	Z = 4
Mo–S		Mo–S	W–S
2.262(2) Å		2.248(3) Å	2.259(3) Å
2.265(2) Å		2.268(4) Å	2.264(4) Å
2.266(2) Å		2.272(5) Å	2.278(3) Å
S–Mo–S		S–Mo–S	S–W–S
107.48(9)°		107.0(2)°	107.4(1)°
107.48(9)°		108.2(1)°	108.3(1)°
107.77(9)°		108.3(1)°	108.6(1)°

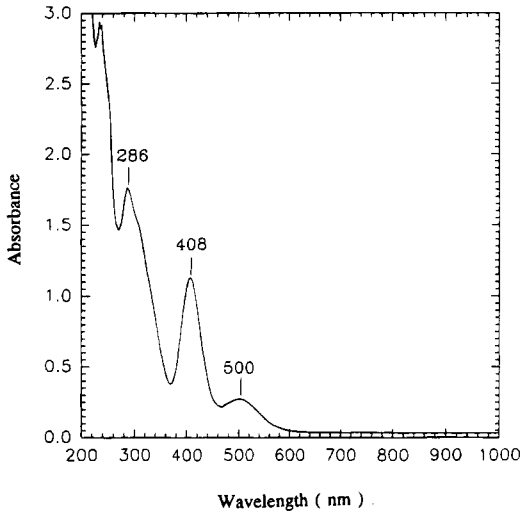

Figure 3. Electronic spectrum of $(n\text{-}Bu_4N)_2[MoOS_3Cu_3BrCl_2]$ in acetonitrile. Concentration 1.49 Mm; optical path 1 mm.

Table 6. Binding Energies of Several Main Elements (eV)

	Mo		Cu		S
	$3d_{5/2}$	$3d_{3/2}$	$2p_{3/2}$	$2p_{1/2}$	2p
$(n\text{-}Bu_4N)_2$-$[MoOS_3Cu_3BrCl_2]$	230.60	233.70	933.10	952.85	162.20
$(NH_4)_2MoOS_3$	230.50	233.50			162.20
CuO			933.50		

bonding in the cluster but also to the future theoretical analysis of the NLO properties of the cluster. Table 6 lists the relevant binding energies of the Mo, Cu, and S atoms in $(n\text{-}Bu_4N)_2[MoOS_3Cu_3BrCl_2]$ measured by XPS.

A +6 oxidation state is assigned to the Mo atom based on the measured binding energy of 230.60 eV ($3d_{5/2}$) and 233.70 eV ($3d_{3/2}$) which are almost identical to the values of 230.50 and 233.50 eV obtained for $(NH_4)_2MoOS_3$ under identical conditions. Apparently, the oxidation state of Mo is not much altered (still +6) upon formation of the $Cu(S)_2Mo$ ring. Compared to CuO, the Cu of the cluster shows a lower binding energy and does not have satellite peaks in the 2p electron level. Thus, we assign its oxidation state to be +1.

Given the relatively high stability of the $[MoOS_3Cu_3BrCl_2]^{2-}$ anion in solution, its well-defined structure and oxidation state, and interesting NLO properties, it became rather intriguing to vary the oxidation state of the cluster and to manipulate the NLO properties by reducing or oxidizing the cluster. In this connection, we studied the cyclic voltammogram of the cluster.

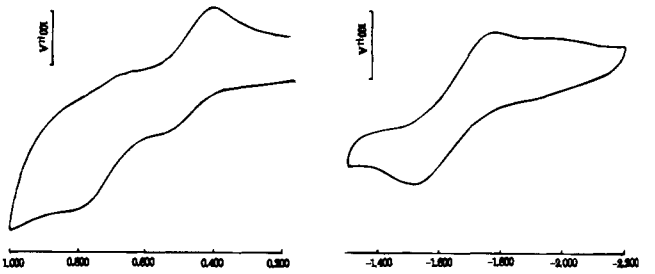

Figure 4. Cyclic voltammogram of $(n\text{-}Bu_4N)_2[MoOS_3Cu_3BrCl_2]$ in acetonitrile containing 0.1 M Et_4NClO_4 as supporting electrolyte.

Unfortunately, the cluster is unstable toward oxidation and reduction (see Figure 4).

The cyclic voltammogram of $(n\text{-}Bu_4N)_2[MoOS_3Cu_3BrCl_2]$ contains only two quasi-reversible redox couples (E_{pa1} = 0.40 V and E_{pc1} = 0.51 V; E_{pa2} = −1.75 V and E_{pc2} = −1.53 V). We believe that the E_{pa1} wave is associated with the Cu, whereas the E_{pa2} wave is associated with the Mo atom.

Nonlinear Refraction and Optical Limiting. Our earlier study showed that cage-shaped clusters $(n\text{-}Bu_4N)_3[MM'_3BrX_3S_4]$ exhibit very large nonlinear absorption and only very small nonlinear refraction (self-focusing).[5,6,12] Over a wide range of compositional variation of M = Mo and W, M′ = Ag and Cu, X = Cl, Br, and I, such a pattern of nonlinear optical behavior is preserved. However, if the cluster structure is changed from a cubic cage shape to a nest shape, two dramatic changes in the NLO property of the cluster will occur: (1) the nonlinear refractive effect becomes much larger; (2) the nature of the nonlinear refractive effect changes from self-focusing to self-defocusing. Structurally, a nest-shaped (nido-) cluster $[MoOS_3Cu_3BrCl_2]^{2-}$ differs only slightly from a cubic cage-shaped (closo-) cluster $[MoCu_3BrCl_3S_4]^{3-}$. (The coordination environments of Mo and S can be described by S_4 and $MoCu_2$ respectively in both cases of $(n\text{-}Bu_4N)_3[MoCu_3BrX_3S_4]$ and $(Et_4N)_2[MoCu_3BrCl_2S_4]$). Yet the contrast between their NLO behavior is distinct.

The earliest evidence of the presence of such a structure/NLO property correlation was collected in the study of $(n\text{-}Bu_4N)_2[MoCu_3OS_3(NCS)_3]$.[7] Studies of the synthesis and NLO properties of the twin-nest-shaped

(12) Unpublished results. When Z-scan experiments were performed on this group of clusters under a closed aperture configuration, only slightly distorted symmetric (with respect to the focal point of the laser beam) Z-scan curves were obtained.

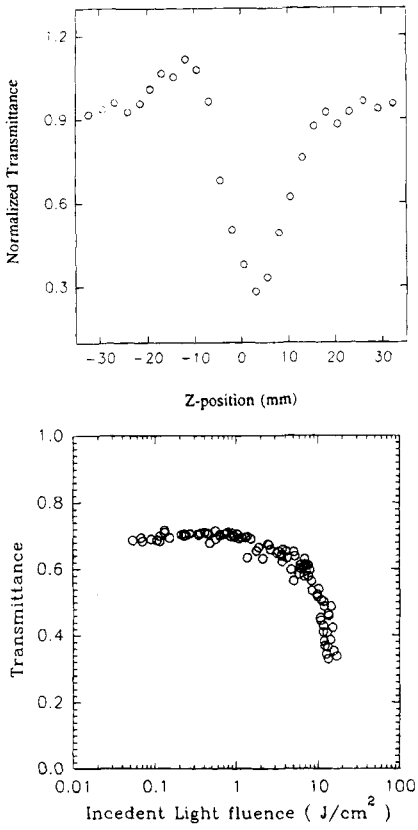

Figure 5. (a) *Z*-scan data collected under closed aperture configuration showing the self-defocusing effect of the cluster, $(n\text{-}Bu_4N)_2[MoOS_3Cu_3BrCl_2]$. (b) Optical limiting effect of the cluster.

cluster $(Et_4N)_4[Mo_2O_2S_6Cu_6Br_2I_4]$ confirmed the existence of this correlation.[8] The synthesis, structural characterization, and NLO study of the title cluster made it even more definitive that it is the cage or nest structural type (not the difference in peripheral ligand sets) that dictates the NLO behavior of the clusters. The large self-defocusing effect[13] of the cluster $(n\text{-}Bu_4N)_2[MoOS_3Cu_3BrCl_2]$ is clearly shown in Figure 5a. It seems certain that the structure alternation of cubic cage ⇄ nest (or closo ⇄ nido) could induce a switch of NLO behavior: nearly pure nonlinear absorption ⇄ containing significant component of nonlinear refraction, and self-focusing ⇄ self-defocusing.

In addition to the light-induced refractive index change as manifested in Figure 5a, $(n\text{-}Bu_4N)_2[MoOS_3Cu_3BrCl_2]$ also exhibits strong nonlinear absorption at 532 nm. The combination of the self-defocusing and nonlinear absorption makes the cluster an interesting candidate for optical limiting applications.[14] The optical limiting capability of the compound $(n\text{-}Bu_4N)_2[MoOS_3Cu_3BrCl_2]$ is demonstrated in Figure 5b. The light energy transmitted starts to deviate from Beer's law as the input light fluence reaches about 1 J/cm^2, and the materials become increasingly less transparent as the light fluence rises. The saturation fluence transmitted is ~10 J/cm^2.

Supplementary Material Available: Crystallographic data for the title compound (9 pages); observed and calculated structure factors (13 pages). Ordering information is given on any current masthead page.

CM940290G

(13) Sheik-Bahae, M.; Said, A. A.; Van Stryland, E. W. *Opt. Lett.* **1989**, *14*, 955.

(14) See, for example: (a) *Conference on Lasers and Electro-Optics*; 1993, Vol. 11, OSA technical digest series; Optical Society of America: Washington, D.C., 1993; pp 614–621. (b) Soileau, M. J., Ed. *Proc. Soc. Photo-Opt. Instrum. Eng.* **1989**, *1105*.